Oncoprotein Akt/PKB induces trophic effects in murine models of Parkinson's disease

Vincent Ries*, Claire Henchcliffe*, Tatyana Kareva*, Margarita Rzhetskaya*, Ross Bland†, Matthew J. During‡, Nikolai Kholodilov*, and Robert E. Burke*§¶

Departments of *Neurology and §Pathology, Columbia University College of Physicians and Surgeons, New York, NY 10032; and †Neurologix Research and ‡Human Cancer Genetics Program, Ohio State University Comprehensive Cancer Center, Columbus, OH 43210

Edited by Solomon H. Snyder, Johns Hopkins University School of Medicine, Baltimore, MD, and approved October 11, 2006 (received for review July 27, 2006)

Despite promising preclinical studies, neurotrophic factors have not yet achieved an established role in the treatment of human neurodegenerative diseases. One impediment has been the difficulty in providing these macromolecules in sufficient quantity and duration at affected sites. An alternative approach is to directly activate, by viral vector transduction, intracellular signaling pathways that mediate neurotrophic effects. We have evaluated this approach in dopamine neurons of the substantia nigra, neurons affected in Parkinson's disease, by adeno-associated virus 1 transduction with a gene encoding a myristoylated, constitutively active form of the oncoprotein Akt/PKB. Adeno-associated virus Myr-Akt has pronounced trophic effects on dopamine neurons of adult and aged mice, including increases in neuron size, phenotypic markers, and sprouting. Transduction confers almost complete protection against apoptotic cell death in a highly destructive neurotoxin model. Activation of intracellular neurotrophic signaling pathways by vector transfer is a feasible approach to neuroprotection and restorative treatment of neurodegenerative disease.

apoptosis | dopamine | neurotrophic | programmed cell death | substantia nigra

Parkinson's disease (PD) is a major public health problem in the world, with an estimated 1,000,000 individuals affected in the United States alone (1). It is a chronic, progressive neurodegenerative disorder that typically manifests with impairments of motor function, including tremor, rigidity, slowness of movement, and poor postural stability, attributable to the loss of dopamine (DA) neurons of the substantia nigra (SN) of the midbrain. These motor manifestations can be treated successfully for a limited period, either with drugs, which restore dopaminergic function, or more recently by deep brain stimulation. However, there is no treatment that forestalls deterioration attributable to progressive neurodegeneration.

For neurodegenerative diseases, one approach that has held promise for providing both neuroprotection and restoration is the administration of protein neurotrophic factors. In PD, substantial effort has been made to explore the possibility of providing neuroprotection and restoration by the intracerebral administration of glial cell line-derived neurotrophic factor (GDNF) (2). A pilot study of intracerebral infusion of GDNF offered promise (3), but a subsequent, larger, double-blind trial failed to demonstrate benefit (4). Although there are many possible reasons for this discrepancy, it is likely that the technical difficulties inherent in reliably providing sufficient quantities of neurotrophic protein within brain parenchyma of affected regions plays a role. These technical constraints apply to the use of other neurotrophic factors in other neurodegenerative diseases as well (5).

An alternative to delivering neurotrophic protein molecules within brain extracellular space is to directly activate the intracellular signaling pathways responsible for their effects. This activation is possible by viral vector approaches to transduction of neurons (6). One such intracellular pathway utilizes the phosphatidylinositide 3′-OH kinase and Akt/PKB signaling cascade (7, 8). In neurons, Akt activation has been identified in response to treatment with insulin-like growth factor 1 (9), nerve growth factor (10), and glial cell line-derived neurotrophic factor (11). Akt signaling mediates two principal cellular responses to neurotrophic factors. It maintains viability through antiapoptotic effects [reviewed in Brunet *et al*. (12)], and it mediates effects on axonal caliber, branching (13), and regeneration (14). Almost all of these observations, however, have been made *in vitro*, and it has not been known whether they generalize to the *in vivo* context, particularly in the central nervous system. We therefore have examined whether Akt mediates trophic effects on adult normal, neurotoxin-lesioned, and aged DA neurons of the SN by adeno-associated virus (AAV)-mediated transduction with a myristoylated (Myr), constitutively active form (15).

Results

Expression of Endogenous Akt Isoforms in SN. We examined expression of endogenous Akt mRNA and protein in the SN (Fig. 5, which is published as supporting information on the PNAS web site). Of the three Akt isoforms, Akt1 mRNA was the most abundantly expressed in SN. At a regional level, Akt1 mRNA was most highly expressed in the SN pars compacta (SNpc), and, at a cellular level, it was expressed exclusively within neurons (data not shown). The same was true for the Akt2 and Akt3 isoforms. The developmental pattern of expression of Akt1 mRNA within SN differed from that observed in striatum and cortex, in that it was relatively sustained in adulthood, at levels 80% of those at postnatal day (PND) 2 (Fig. 5*C*). In striatum and cortex, mRNA levels in adulthood were ≈40% of those at PND2. At the protein level, phospho-Akt(Ser-473) was detected within the SNpc and specifically within DA neurons (Fig. 5*D*).

Trophic Effects of AAV Myr-Akt in Normal Adult Mice. Transduction of neurons of the SN of adult male mice with AAV Myr-Akt induced a 50% increase in nigral volume (Fig. 1*A*). At a cellular level, for the SNpc, this increased regional volume was attributable, in part, to a 50% increase in neuron size (Fig. 1*B*). There was, in addition, a 44% increase in the number of tyrosine hydroxylase (TH)-positive neurons (Fig. 1*C*). We attribute this

Author contributions: V.R., C.H., M.J.D., N.K., and R.E.B. designed research; V.R., C.H., T.K., M.R., R.B., and N.K. performed research; V.R., C.H., and R.E.B. analyzed data; and V.R., C.H., R.B., M.J.D., N.K., and R.E.B. wrote the paper.

The authors declare no conflict of interest.

This article is a PNAS direct submission.

Freely available online through the PNAS open access option.

Abbreviations: AAV, adeno-associated virus; PD, Parkinson's disease; DA, dopamine; SN, substantia nigra; Myr, myristoylated; SNpc, SN pars compacta; TH, tyrosine hydroxylase; HVA, homovanillic acid; 6OHDA, 6-hydroxydopamine.

¶To whom correspondence should be addressed at: Department of Neurology, Room 306, Black Building, Columbia University Medical Center, 650 West 168th Street, New York, NY 10032. E-mail: rb43@columbia.edu.

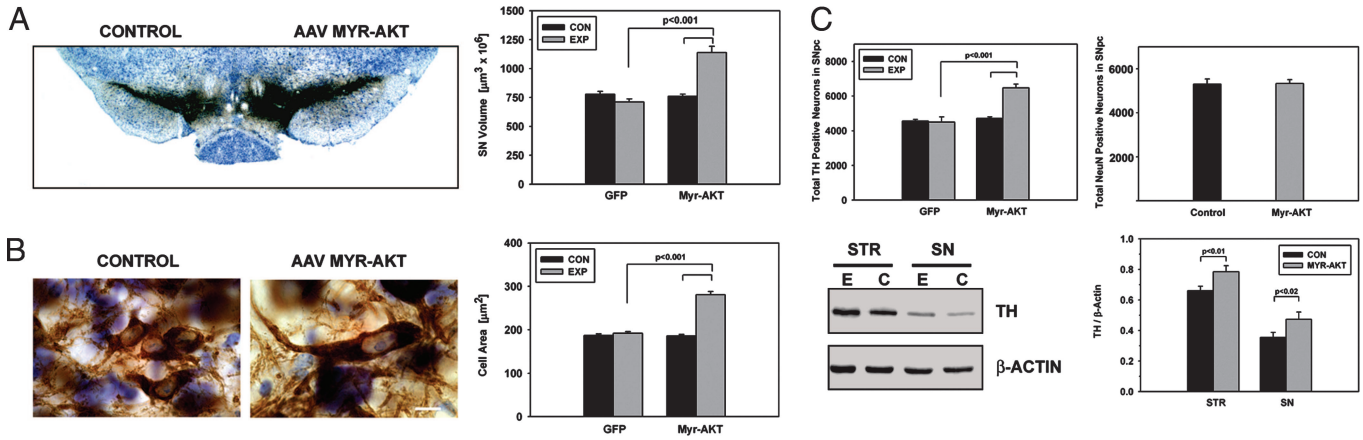

Fig. 1. Trophic effects of Myr-Akt on DA neurons of the SN in adult mice. (*A*) A section processed for TH immunostaining and thionin counterstain at 7 weeks after AAV Myr-Akt injection demonstrates an increase in the size of the SN and the SNpc. The volume of the injected (EXP, experimental) SN was 1,139.2 ± 54.1 ($\times 10^6$) μm^3 (mean ± SEM), a 50% increase in comparison to the contralateral, noninjected control (CON) side (760.6 ± 18.5 ($\times 10^6$) μm^3) ($P < 0.001$; $n = 6$ animals for Myr-Akt and GFP groups). (*B*) At a cellular level, the increased volume of the SNpc was attributable, at least in part, to an increase in the size of DA neurons. (Bar: 10 μm.) The cross-sectional areas of the TH-positive neurons in the SNpc of Myr-Akt-injected mice was 281.2 ± 7.1 μm^2 (mean ± SEM), a 50% increase in comparison to the contralateral, noninjected control side (185.5 ± 3.3 μm^2) ($P < 0.001$; $n = 2$ mice for both GFP control and Myr-Akt; $n = 50$ neurons in all conditions). (*C*) The increase in the volume of the SNpc also was accompanied by an increase in the number of TH-positive neurons. In the AAV Myr-Akt-injected SN, there was a mean of 6,483 ± 204 neurons, a 44% increase in comparison to the AAV GFP-injected SN (4,504 ± 295) ($P < 0.001$, ANOVA; $n = 6$ animals in both groups). Counts of total SNpc neurons, determined as stereologic counts of NeuN-stained profiles were unchanged (*Right*) ($n = 4$ animals). An increased level of TH expression in the SN after AAV Myr-Akt was demonstrated by Western analysis, as shown in *Lower Left*, and in a quantitative analysis of TH band optical densities normalized for β-actin ($n = 5$ animals). An increase in TH protein expression also was observed in striatum (STR) (E, experimental, AAV Myr-Akt-injected side; C, control, contralateral side).

apparent increase in DA neuron number to an increased level of expression of TH, determined by Western blotting analysis (Fig. 1*C*), and a resulting increase in detection by immunostaining, rather than an actual increase in the number of neurons, because counts of neuronal profiles in the SNpc, detected by NeuN immunostaining, were unchanged (Fig. 1*C*). These morphologic changes were accompanied by changes in the levels of DA (137% increase above AAV GFP control), and its metabolites homovanillic acid (HVA) (148% increase) and 3,4-dihydroxyphenylacetic acid (DOPAC) (35% increase) (Fig. 6, which is pub-

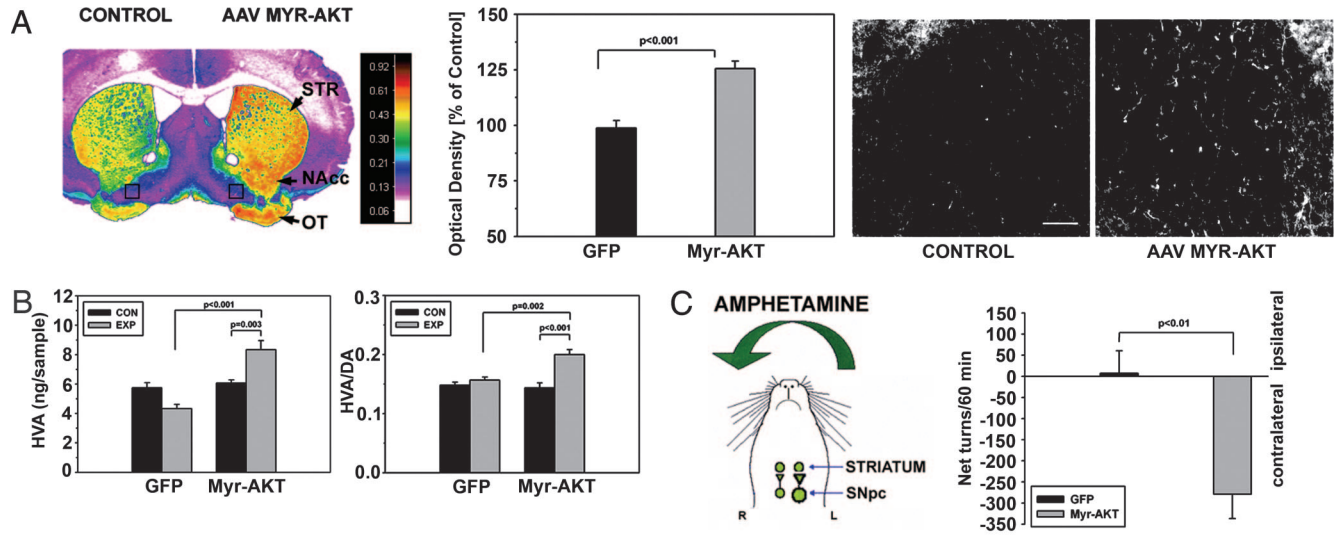

Fig. 2. Trophic effects of Myr-Akt on the axonal projections of SN DA neurons. (*A*) (*Left*) A pseudocolor image of a coronal section through the striatum, processed for TH immunostaining at 7 weeks after intranigral AAV Myr-Akt injection, reveals higher density values (red-orange) in the striatum (STR) on the injected side. Higher-density values also are observed in the nucleus accumbens (NAcc) and olfactory tubercle (OT). (*Center*) An increase in the optical density of the striatal TH immunostaining is shown quantitatively as a 26% increase over values for the contralateral, noninjected striatum; this was a highly significant increase in comparison to AAV GFP-injected animals ($P < 0.001$, *t* test; $n = 6$ animals for both groups). (*Right*) At a cellular level, this increase in optical density was attributable to an increase in the number and caliber of TH-positive fibers. (Bar: 50 μm.) The regions shown in these micrographs are between the accumbens and olfactory tubercle on both sides of the section (indicated as black rectangles in *Left*). (*B*) These morphologic changes were accompanied by biochemical changes indicative of increased DA release in the striatum. There was an increase in both HVA ($P < 0.001$) and the HVA/DA ratio ($P = 0.002$, ANOVA, AAV Myr-Akt-injected side compared with AAV GFP-injected side; $n = 6$ animals in each group) (EXP, experimental, injected side; CON, control, noninjected side). (*C*) (*Left*) When AAV Myr-Akt-injected mice were administered amphetamine (5 mg/kg i.p.), they exhibited rotational behavior contraversive to the side of the vector injection. (*Right*) Contraversive rotations are plotted as negative net rotations. AAV GFP-injected mice did not demonstrate such behavior.

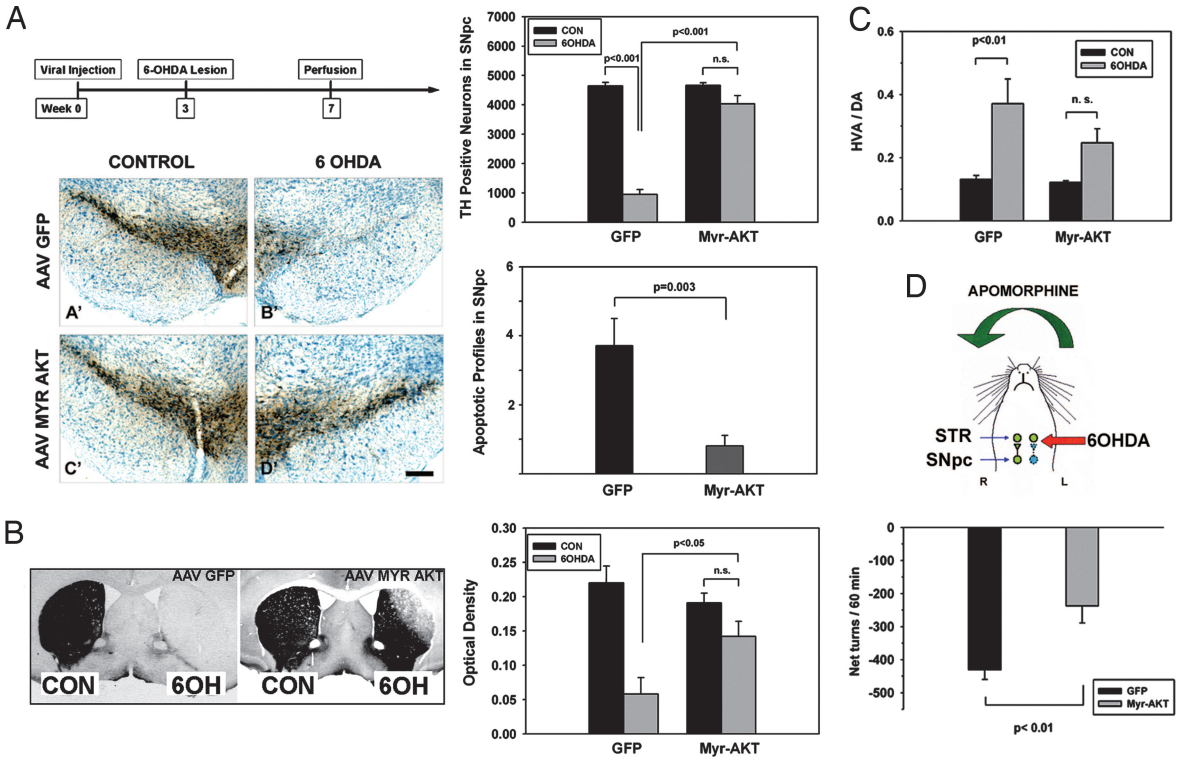

Fig. 3. Neuroprotective effects of Myr-Akt in the intrastriatal 6OHDA mouse model. (*A*) (*Left Upper*) The chronic morphologic studies shown in *A* and *B* were performed according to the timeline shown. The studies of apoptosis were conducted at 6 days after 6OHDA. (*Left Lower*) Mice treated with an AAV GFP control injection show an almost complete loss of TH-positive SNpc neurons. This loss is almost completely prevented in mice injected with AAV Myr-Akt (*D'*). (Bar: 200 μm.) (*Right Upper*) This effect is shown quantitatively as stereologic counts of the number of surviving TH-positive neurons. In mice given AAV GFP, TH-positive neuron numbers were reduced to 950 $\pm$ 163 after 6OHDA injection, or 20% of the noninjected contralateral control (CON) (4,646 $\pm$ 119). In mice given AAV Myr-Akt, neuron numbers were reduced to only 4,036 $\pm$ 280, or 87% of the contralateral control (4,664 $\pm$ 85). The difference between the AAV GFP and AAV Myr-Akt groups was highly significant ($P < 0.001$, ANOVA; $n = 6$ animals GFP; $n = 7$ animals Myr-Akt). (*Right Lower*) This protective effect of Myr-Akt on SNpc DA neurons was attributable to suppression of apoptosis as shown. The number of apoptotic profiles in the SNpc was reduced to 22% of the number observed in AAV GFP-treated mice ($P = 0.003$, *t* test; $n = 7$ animals AAV GFP; $n = 8$ animals AAV Myr-Akt). (*B*) The neuroprotective effect of Myr-Akt was observed at the level of the striatal axonal projections as well. (*Left*) In control AAV GFP-injected mice, there is an almost complete loss of striatal TH-positive staining on the 6OHDA-injected side. In AAV Myr-Akt-injected mice, there is some loss of immunoperoxidase labeling in the dorsolateral quadrant of the injected striatum, but otherwise staining of TH fibers is preserved. The mice used for this analysis were the same as those used for the stereologic analysis in *A*. (*Right*) The protective effect of Myr-Akt on striatal TH-positive fibers is shown quantitatively as optical densities of TH staining. (*C*) The morphologic preservation of striatal dopaminergic fibers was accompanied by relative preservation of biochemical indices of dopaminergic terminals. At 4 weeks after 6OHDA, striatal DA levels in AAV Myr-Akt-treated mice were 19.8 $\pm$ 4.2 ng per sample, a 3.4-fold increase over the mean value of 5.8 $\pm$ 2.9 observed in AAV GFP-treated mice ($P < 0.03$; $n =$ 6 animals AAV GFP; $n = 8$ animals AAV Myr-Akt) (data not shown). HVA levels were increased by 3-fold (data not shown). After lesions of the nigrostriatal dopaminergic projection, there is a compensatory increase in DA turnover, reflected in an increased HVA/DA ratio (16). This effect was observed in AAV GFP-treated mice as an increase in the HVA/DA ratio from 0.13 $\pm$ 0.01 in the nonlesioned striatum to 0.37 $\pm$ 0.08 in the lesioned striatum ($P = 0.006$). However, in the AAV Myr-Akt-treated mice, although there was a trend for this effect, it did not achieve significance. (*D*) To assess functionality of the nigrostriatal projection we examined apomorphine-induced rotations. After partial destruction of the dopaminergic projection, postsynaptic supersensitivity to direct-acting DA agonists, such as apomorphine, results in contraversive rotations (29). Strong contraversive rotational behavior was observed in AAV GFP-treated mice after apomorphine injection (0.5 mg/kg) at 4 weeks after 6OHDA lesion. This contraversive rotational behavior was significantly diminished in mice treated with AAV Myr-Akt (AAV GFP, -431 ± 29 net turns per 60 min; AAV Myr-Akt, -237 ± 52; $P = 0.006$, *t* test; $n = 7$ animals GFP; $n = 6$ animals Myr-Akt).

lished as supporting information on the PNAS web site). The increase in neuron size was not confined to DA neurons. Nondopaminergic neurons of the SN pars reticulata also were increased by 76% (control, noninjected SNpr: 177 $\pm$ 7 μm^2; AAV Myr-Akt: 312 $\pm$ 13 μm^2; $n = 2$ mice; 40 neurons total; $P <$ 0.001).

These trophic effects at the level of DA neuron cell bodies were accompanied by effects in their axonal projections within the striatum. At 7 weeks after intranigral injection of AAV Myr-Akt, there was an increased density of TH-immunoreactive fibers within the ipsilateral striatum (Fig. 2*A*). At a cellular level, although some of this increase in staining density could be attributed to an induction of TH protein expression (Fig. 1*C*), there also was a clear induction of fiber sprouting (Fig. 2*A*). In addition, the caliber of fibers was increased by 37% (contralateral control: 1.6 $\pm$ 0.1 μm; AAV Myr-Akt: 2.2 $\pm$ 0.1 μm; $P <$ 0.001; paired *t* test; $n = 3$ mice; 30 fibers in both control and Myr-Akt conditions) (Fig. 2*A*). There was increased striatal DA turnover ipsilateral to the side of the AAV Myr-Akt injection, reflected in higher levels of HVA (Fig. 2*B*) and a higher HVA/DA ratio (Fig. 2*B*). Although AAV Myr-Akt-injected mice showed no apparent behavioral motor asymmetries, they did show augmented contraversive rotations after amphetamine injection (Fig. 2*C*), indicating that the sprouting of dopaminergic fibers within the striatum was accompanied by an increased functional capacity to release DA.

Neuroprotective Effects of AAV Myr-Akt in a Neurotoxin Model. In addition to these trophic effects, AAV Myr-Akt was protective in a neurotoxin model of PD. Injection three weeks before intrastriatal 6-hydroxydopamine (6OHDA) conferred near complete protection of DA neuron cell bodies. Although there was

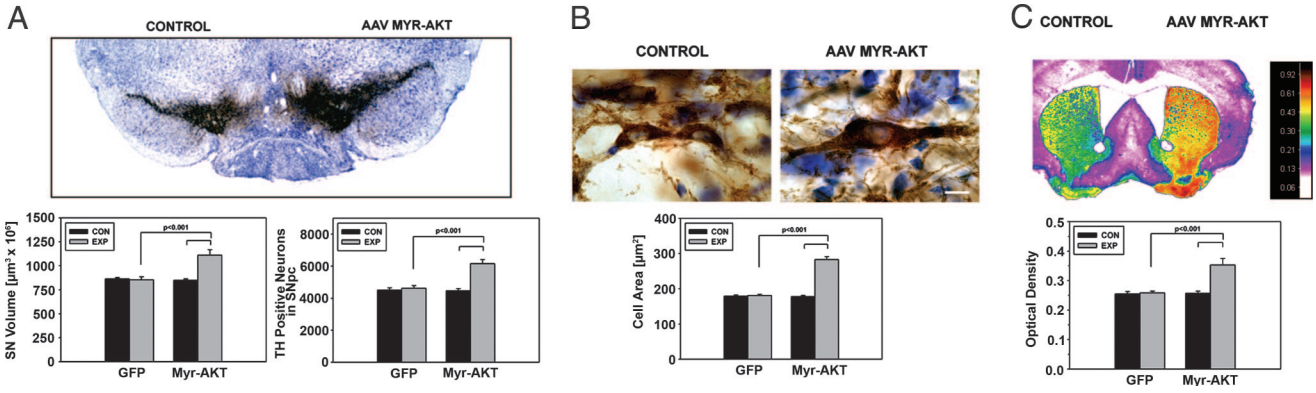

Fig. 4. Trophic effects of Myr-Akt on DA neurons of the SN in aged mice. (*A*) Aged mice were injected with either AAV GFP or AAV Myr-Akt and killed for morphologic analysis 7 weeks later. Myr-Akt induced a 31% increase in the total volume of the SN as compared with the contralateral noninjected SN. There also was an increase in the number of TH-positive neurons; the AAV Myr-Akt-injected SN contained 6,158 ± 253 neurons, a 38% increase above the number of 4,467 ± 131 on the contralateral control side ($P < 0.001$, Tukey's test; $n = 6$ animals). (*B*) As in young mice, Myr-Akt induced an increase in the size of individual TH-positive neurons, as shown. (Scale bar: 10 μm.) (*C*) As in young mice, sprouting was observed with a 37% increase in TH optical density values on the AAV Myr-Akt-injected side in comparison to contralateral control and both striata of AAV GFP-injected mice ($P < 0.001$, Tukey).

a trend for neuron loss on the 6OHDA-injected side (4,036 ± 280 neurons per SN), it was not significantly different from the noninjected control side (4,664 ± 86). This number of neurons represents a more than 4-fold increase over the surviving number in AAV GFP control-injected animals (950 ± 163) (Fig. 3*A*). Increased survival in DA neurons was attributed to a suppression of apoptotic death (Fig. 3*A*).

Myr-Akt also provided protection against axonal loss. At 28 days after 6OHDA, striatal TH optical density levels were reduced only 26% in AAV Myr-Akt-treated mice, whereas they were reduced 74% in AAV GFP-injected controls (Fig. 3*B*) ($P < 0.05$). This morphologic preservation of the dopaminergic striatal projection was accompanied by preservation of biochemical measures of DA and HVA (data not shown). In addition, although the 6OHDA lesion in AAV GFP control mice resulted in an increased rate of DA turnover, indicated by an increased HVA/DA ratio, as previously reported (16), this effect was diminished in the AAV Myr-Akt-injected mice (Fig. 3*C*). This morphologic and biochemical preservation of striatal dopaminergic fibers was functionally significant, because it was associated with diminished apomorphine-induced contraversive rotations, which are attributable to dopaminergic denervation-induced receptor supersensitivity (Fig. 3*D*). The preservation of striatal dopaminergic fibers was a lasting effect, because at 60 days after lesion, density levels were reduced only by 39% in Myr-Akt-treated animals, whereas in GFP controls, they were reduced by 83% ($P < 0.001$) (data not shown).

Although the above experiments demonstrate an ability of Myr-Akt to protect DA neuron cell bodies and axons when given before the neurotoxin, they do not test its effect in circumstances in which dopaminergic dysfunction occurs before therapeutic intervention, as is the clinical situation in PD. To assess Myr-Akt in a paradigm that better simulates the clinical context, we first administered 6OHDA intrastriatally and waited 3 weeks before intranigral injection of AAV Myr-Akt, at which time it is anticipated that ≈40–50% of SN DA neurons remain (Fig. 7, which is published as supporting information on the PNAS web site). In this paradigm, the number of surviving TH-positive neurons at 7 weeks after AAV Myr-Akt injection was 50% of the contralateral control number, whereas the number in AAV GFP-injected controls was reduced to 14% ($P < 0.001$) (Fig. 7). Striatal dopaminergic terminals also were relatively preserved in the Myr-Akt-treated group (Fig. 7).

Trophic Effects of AAV Myr-Akt in Aged Mice. The principal risk factor for PD is increased age (17), and atrophic changes occur in dopaminergic neurons with age (18). We therefore sought to determine whether Myr-Akt has trophic effects on dopaminergic neurons of aged mice. In 22-month-old aged mice, Myr-Akt produced a 31% increase in the volume of the SN (Fig. 4*A*). As in young mice, this effect for the SNpc was attributable, at least in part, to a 60% increase in average neuronal size (Fig. 4*B*). There also was an increase in the number of TH-positive SN dopaminergic neurons (Fig. 4*A*). These neuron size and number effects were not significantly different from those observed in young mice. Aged mice also demonstrated a sprouting response of dopaminergic axons in response to Myr-Akt (Fig. 4*C*), a difference somewhat greater than that observed in young mice but not significantly. We conclude that for most measures, aged mice are as responsive to Myr-Akt as young mice are.

Discussion

These results demonstrate the feasibility of using viral vector transfer to induce trophic responses in normal adult and aged neurons of the central nervous system by direct activation of the intracellular pathways that mediate responses to extracellular neurotrophic molecules. We used an N-terminal Myr form of the survival signaling kinase Akt, which is constitutively targeted to plasma cell membrane and activated (15). This form of Akt had multiple trophic effects on DA neurons of the SN, including (*i*) an increase in neuron size, (*ii*) an increase in the level of expression of TH, and (*iii*) a sprouting response in dopaminergic axons, associated with a functional behavioral correlate.

A number of these effects are in keeping with prior observations on phosphatidylinositide 3′-OH kinase and Akt signaling. Akt signaling previously has been shown to regulate cell size in pancreatic islet cells (19) and cardiac myocytes (20). For neurons, it has been shown that null mutations in PTEN, a negative regulator of phosphatidylinositide 3′-OH kinase-Akt signaling, results in macrocephaly with an increase in neuron soma size (21). Conversely, null mutation of the Akt3 isoform results in smaller brain size attributable to smaller cells (22). However, all of these observations were made in mice with genetic alteration of the germ line, so that the induced mutations were operative throughout development. Our observations are the first to demonstrate the ability of Akt to regulate neuron size in the mature and even aged nervous system.

Akt also has been demonstrated to regulate axonal growth. In culture, Akt expression modifies axon branching of peripheral sensory neurons (13), and, *in vivo*, it regulates the rate of regeneration of peripheral motor nerves after axotomy (14). We

demonstrate here in the central nervous system that Akt also regulates axon sprouting in both adult and aged animals, either in the presence or absence of injury. In both contexts, induced sprouting results in functionally competent nerve endings, because in both normal and 6OHDA-lesioned animals, the Akt-induced increase in dopaminergic striatal innervation had behavioral correlates.

In addition to these trophic effects on normal adult and aged DA neurons, Myr-Akt also demonstrated an ability to block apoptosis in a potent neurotoxin model of parkinsonism, that induced by intrastriatal injection of 6OHDA. We selected this model for several reasons. First, 6OHDA is an endogenous metabolite of DA (23), having been detected in human caudate (24). Thus, to the extent that oxidative metabolism of endogenous DA may play a role in human PD (reviewed in ref. 25), 6OHDA may model this process. Second, among models of PD associated with SN DA neuron death, intrastriatal 6OHDA has been demonstrated unequivocally to induce apoptosis (26). Third, among PD models, the 6OHDA model is the most destructive, typically resulting in over 80% loss of SN DA neurons. And finally, in this model, SN DA neuron loss is progressive (27), like the human disease. The suppression of apoptosis in this model afforded by Myr-Akt was both substantial and lasting, as indicated by an almost complete preservation of the population of SN DA neurons at 28 days after toxin injection. In this respect, Myr-Akt differs from a number of other neuroprotective approaches that suppress cell death in the acute injury period but do not offer increases in DA neuron survival in the long term (28).

To better simulate the clinical setting, we assessed the effects of AAV Myr-Akt-injected at 3 weeks after 6OHDA, by which time ≈50% of DA neurons are lost (27). There was a 50% survival of DA neurons, assessed 10 weeks after 6OHDA (Fig. 7). Although our data are not directly comparable to those of Sauer and Oertel (27), because of species differences, we estimate that in this paradigm AAV Myr-Akt provided substantial protection of remaining viable neurons. In contrast, AAV GFP-injected controls had only 14% neurons surviving at this time point, a near 4-fold reduction.

In addition to its ability to protect DA neuron cell bodies, AAV Myr-Akt also demonstrated an ability to preserve axonal projections, with preservation of both morphologic and biochemical indices of the dopaminergic projection. Function also was preserved as demonstrated by the reduction of apomorphine-induced rotations after 6OHDA. Apomorphine-induced rotations in the 6OHDA model are attributed to the development of postsynaptic DA receptor supersensitivity after disruption of the nigro-striatal projection (29). Therefore, reduction of rotational behavior suggests that supersensitivity has been diminished by partial restoration of striatal DA release in the AAV Myr-Akt-treated animals. This ability of AAV Myr-Akt to preserve the dopaminergic axonal projection distinguishes it as a neuroprotective approach from many others based on blockade of apoptosis that preserves cell bodies but not axonal projections (30).

The relatively sustained expression of Akt1 mRNA, the most abundant isoform in SN, into adulthood, and the marked trophic effects of constitutively active Akt on adult and aged DA neurons suggest the possibility that endogenous Akt may normally play a role in maintaining viability or functionality of these neurons. Such a possibility is of interest in relation to recent observations on DJ-1 (PARK7), in which loss-of-function mutations result in human PD (31). DJ-1 has been shown in *Drosophila* to function as a suppressor of PTEN, a negative regulator of Akt signaling (32). Consistent with these observations, inhibition of DJ-1A in *Drosophila* by RNA interference results in reduced phosphorylation of Akt and degeneration of DA neurons (33). Thus, Akt signaling may be an important molecular mechanism in the pathogenesis of familial PD.

The ability of AAV Myr-Akt to provide neuroprotection in a potent neurotoxin model of PD, particularly its ability to preserve both dopaminergic cell bodies and axonal projections even when administered 3 weeks after the neurotoxin, suggests that it may provide a previously uncharacterized approach to gene therapy in PD. However, Akt is a potent oncogene, and although we did not observe neoplasia in any of the brains examined as long as 81 days after viral injection, it remains possible that chronic expression of a constitutively active form, particularly in nonneuronal brain cells, carries a risk of neoplastic transformation. Nevertheless, with the development of cell-specific expression systems for DA neurons, coupled to the neuronal tropism of AAV, it should be possible to explore the clinical use of Myr-Akt and other factors affecting its function for the treatment of PD.

Methods

Generation of a Recombinant AAV. A plasmid encoding a 5′ src myristoylation signal in frame with mouse Akt1 was kindly provided by Thomas Franke (Columbia University) (34, 35). (Detailed characterization can be found in *Supporting Text*, which is published as supporting information on the PNAS web site.) The Myr-Akt sequence was modified to incorporate a FLAG-encoding sequence at the 3′ end and inserted into an AAV packaging construct as previously described (36). The genomic titer of each virus ranged from 6.1×10^{12} to 1.2×10^{13} viral genomes per ml. Enhanced GFP was subcloned into the same viral backbone, and viral stocks were used at a titer of $4.6–9.1 \times 10^{12}$.

Experimental Animals. Adult (8-week-old) male C57BL/6 mice were obtained from Charles River Laboratories (Wilmington, MA). Aged male mice (22 months old) were obtained through the National Institute on Aging (Bethesda, MD). For studies of developmental expression of Akt, postnatal rats were used. All injection procedures, described below, were approved by the Columbia University Animal Care and Use Committee.

Virus Injection. Mice were anesthetized with ketamine/xylazine solution and placed in a stereotaxic frame (Kopf Instruments, Tujunga, CA). The tip of 5.0-μl syringe (Agilent, Santa Clara, CA) needle (26S) was inserted to stereotaxic coordinates: AP, −0.35 cm; ML, +0.11 cm; and DV, −0.37 cm, relative to bregma. Viral vector suspension in a volume of 2.0 μl was injected at 0.1 μl/min over 20 min. Characterization of the viral injections is presented in the *Supporting Text*. See Fig. 8, which is published as supporting information on the PNAS web site, for histologically confirmed transduction of DA neurons of the SN with AAV Myr-Akt.

6OHDA Lesion. Adult mice received a unilateral intrastriatal injection of 6OHDA as described in ref. 28 and as detailed in *Supporting Text*.

Immunohistochemistry. Immunostaining for TH was performed as described in ref. 37 and as detailed in *Supporting Text*. Procedures for immunostaining of the FLAG epitope and phosphorylated Akt are described in detail in *Supporting Text*.

Determination of SN DA Neuron Numbers by Stereologic Analysis. Stereologic analysis was performed under blinded conditions on coded slides. For each animal, the SN on both sides of the brain was analyzed. For each section, the entire SN was identified as the region of interest. With StereoInvestigator software (MicroBright Field, Inc., Williston, VT), a fractionator probe was established for each section. The number of TH-positive neurons

in each counting frame then was determined by the optical disector method (38). Further methodologic detail is provided in *Supporting Text*.

Determination of the Number of Apoptotic Profiles Within the SN. Apoptotic profiles were identified in the SN on TH-immunoperoxidase stained and thionin-counterstained sections as previously described (39).

Measurement of SN and Striatal DA and Metabolites. These assays are described in *Supporting Text*.

Western Analysis of TH and the DA Transporter (DAT). These analyses are described in *Supporting Text*.

Behavioral Analysis. Amphetamine-induced rotational behavior in nonlesioned mice was tested at 7 weeks after the viral injection. Mice were injected with amphetamine (5 mg/kg i.p.) (Sigma-Aldrich, St. Louis, MO) and placed free roaming in a plastic hemispherical bowl with a diameter of 26.5 cm. They were allowed to habituate to their environment for 15 min, and then contralateral and ipsilateral turns were counted for 60 min. Results are expressed as net turns per 60 min. Apomorphine-induced rotational behavior was assessed at 4 weeks after lesion. Mice received a s.c. dose of apomorphine (0.5 mg/kg) (Sigma-RBI, Natick, MA), and rotations were monitored by using the same experimental setup as for amphetamine-induced rotation.

Northern and *in Situ* Hybridization Analysis of Akt Isoforms During Development. These analyses are described in *Supporting Text*.

Statistical Methods. Multiple comparisons among groups were performed by one-way analysis of variance and Tukey post hoc analyses.

We thank Ms. Anna Yarygina and Ms. Amy Baohan for morphometric analyses and Dr. Lloyd Greene for his helpful review of the manuscript. This work was supported by National Institutes of Health Grants NS26836, NS38370, and DAMD17-03-1-0492; the Parkinson's Disease Foundation; the Lowenstein Foundation; and the Michael J. Fox Foundation.

1. Mayeux R (2003) *Annu Rev Neurosci* 26:81–104.
2. Lin L-FH, Doherty DH, Lile JD, Bektesh S, Collins F (1993) *Science* 260:1130–1132.
3. Gill SS, Patel NK, Hotton GR, O'Sullivan K, McCarter R, Bunnage M, Brooks DJ, Svendsen CN, Heywood P (2003) *Nat Med* 9:589–595.
4. Lang AE, Gill S, Patel NK, Lozano A, Nutt JG, Penn R, Brooks DJ, Hotton G, Moro E, Heywood P, *et al*. (2006) *Ann Neurol* 59:459–466.
5. Thoenen H, Sendtner M (2002) *Nat Neurosci* 5(Suppl):1046–1050.
6. Davidson BL, Breakefield XO (2003) *Nat Rev Neurosci* 4:353–364.
7. Datta SR, Brunet A, Greenberg ME (1999) *Genes Dev* 13:2905–2927.
8. Kaplan DR, Miller FD (2000) *Curr Opin Neurobiol* 10:381–391.
9. Dudek H, Datta SR, Franke TF, Birnbaum MJ, Yao R, Cooper GM, Segal RA, Kaplan DR, Greenberg ME (1997) *Science* 275:661–665.
10. Soltoff SP, Rabin SL, Cantley LC, Kaplan DR (1992) *J Biol Chem* 267:17472–17477.
11. Creedon DJ, Tansey MG, Baloh RH, Osborne PA, Lampe PA, Fahrner TJ, Heuckeroth RO, Milbrandt J, Johnson EMJ (1997) *Proc Natl Acad Sci USA* 94:7018–7023.
12. Brunet A, Datta SR, Greenberg ME (2001) *Curr Opin Neurobiol* 11:297–305.
13. Markus A, Zhong J, Snider WD (2002) *Neuron* 35:65–76.
14. Namikawa K, Honma M, Abe K, Takeda M, Mansur K, Obata T, Miwa A, Okado H, Kiyama H (2000) *J Neurosci* 20:2875–2886.
15. Pellman D, Garber EA, Cross FR, Hanafusa H (1985) *Nature* 314:374–377.
16. Zigmond MJ, Abercrombie ED, Berger TW, Grace AA, Stricker EM (1990) *Trends Neurosci* 13:290–296.
17. Bower JH, Maraganore DM, McDonnell SK, Rocca WA (2000) *Mov Disord* 15:819–825.
18. Emborg ME, Ma SY, Mufson EJ, Levey AI, Taylor MD, Brown WD, Holden JE, Kordower JH (1998) *J Comp Neurol* 401:253–265.
19. Tuttle RL, Gill NS, Pugh W, Lee JP, Koeberlein B, Furth EE, Polonsky KS, Naji A, Birnbaum MJ (2001) *Nat Med* 7:1133–1137.
20. Shioi T, McMullen JR, Kang PM, Douglas PS, Obata T, Franke TF, Cantley LC, Izumo S (2002) *Mol Cell Biol* 22:2799–2809.
21. Backman SA, Stambolic V, Suzuki A, Haight J, Elia A, Pretorius J, Tsao MS, Shannon P, Bolon B, Ivy GO, *et al*. (2001) *Nat Genet* 29:396–403.
22. Easton RM, Cho H, Roovers K, Shineman DW, Mizrahi M, Forman MS, Lee VM, Szabolcs M, de Jong R, Oltersdorf T, *et al*. (2005) *Mol Cell Biol* 25:1869–1878.
23. Kostrzewa RM, Jacobowitz DM (1974) *Pharmacol Rev* 26:199–288.
24. Curtius HC, Wolfensberger M, Steinmann B, Redweik U, Siegfried J (1974) *J Chromatogr* 99:529–540.
25. Fahn S, Sulzer D (2004) *NeuroRx* 1:139–154.
26. Marti MJ, Saura J, Burke RE, Jackson-Lewis V, Jimenez A, Bonastre M, Tolosa E (2002) *Brain Res* 958:185–191.
27. Sauer H, Oertel WH (1994) *Neuroscience* 59:401–415.
28. Silva RM, Ries V, Oo TF, Yarygina O, Jackson-Lewis V, Ryu EJ, Lu PD, Marciniak SM, Ron D, Przedborski S, *et al*. (2005) *J Neurochem* 95:974–986.
29. Pycock CJ (1980) *Neuroscience* 5:461–514.
30. Eberhardt O, Coelln RV, Kugler S, Lindenau J, Rathke-Hartlieb S, Gerhardt E, Haid S, Isenmann S, Gravel C, Srinivasan A, *et al*. (2000) *J Neurosci* 20:9126–9134.
31. Bonifati V, Rizzu P, van Baren MJ, Schaap O, Breedveld GJ, Krieger E, Dekker MC, Squitieri F, Ibanez P, Joosse M, *et al*. (2003) *Science* 299:256–259.
32. Kim RH, Peters M, Jang Y, Shi W, Pintilie M, Fletcher GC, DeLuca C, Liepa J, Zhou L, Snow B, *et al.* (2005) *Cancer Cell* 7:263–273.
33. Yang Y, Gehrke S, Haque ME, Imai Y, Kosek J, Yang L, Beal MF, Nishimura I, Wakamatsu K, Ito S, *et al.* (2005) *Proc Natl Acad Sci USA* 102:13670–13675.
34. Franke TF, Yang SI, Chan TO, Datta K, Kazlauskas A, Morrison DK, Kaplan DR, Tsichlis PN (1995) *Cell* 81:727–736.
35. Ahmed NN, Grimes HL, Bellacosa A, Chan TO, Tsichlis PN (1997) *Proc Natl Acad Sci USA* 94:3627–3632.
36. Olson VG, Heusner CL, Bland RJ, During MJ, Weinshenker D, Palmiter RD (2006) *Science* 311:1017–1020.
37. Kholodilov N, Yarygina O, Oo TF, Zhang H, Sulzer D, Dauer WT, Burke RE (2004) *J Neurosci* 24:3136–3146.
38. Coggeshall RE, Lekan HA (1996) *J Comp Neurol* 364:6–15.
39. Oo TF, Kholodilov N, Burke RE (2003) *J Neurosci* 23:5141–5148.